Physics Letters B 813 (2021) 136060

Contents lists available at ScienceDirect

Physics Letters B

www.elsevier.com/locate/physletb

Disk galaxies and their dark halos as self-organized patterns

Shankar C. Venkataramani *, Alan C. Newell

Department of Mathematics, University of Arizona, 617 N. Santa Rita Ave., Tucson, AZ 85721, USA

ARTICLE INFO

Article history:
Received 20 August 2020
Received in revised form 9 November 2020
Accepted 28 December 2020
Available online 30 December 2020
Editor: M. Trodden

Keywords:
Self-organized patterns
Symmetry breaking
Defects
Dark matter
Galaxy scaling relations

ABSTRACT

Galaxies are built by complex physical processes with significant inherent stochasticity. It is therefore surprising that the inferred dark matter distributions in galaxies are correlated with the observed baryon distributions leading to various 'Baryon-Halo conspiracies'. The fact that no dark matter candidate has been definitively identified invites a search for alternative explanations for such correlations and we present an approach motivated by the behaviors of self organized patterns. We propose a nonlocal relativistic Lagrangian theory for a 'pattern field' which acts as an 'effective dark matter', built on the idea that defects in this pattern field couple to the baryonic matter distribution. The model applies to rotation supported systems and, for them, we compute galactic rotation curves, obtain a radial acceleration relation with two branches, and deduce the Freeman limit for central surface brightness.

1. Mass discrepancies and dark matter

Understanding the nature of dark matter is one of the great intellectual challenges of our time. Dark matter is postulated to explain discrepancies between the observed (non-relativistic) motions of stars in galaxies, and galaxies in clusters, from the predictions of Newtonian gravity [1]. Although long suspected [2,3], the hunt for additional 'invisible' matter became a serious endeavor in the wake of the pioneering observations by Vera Rubin and her colleagues [4,5], demonstrating definitively that the rotation velocity curves $v(r)$ of galaxies flatten out with increasing radius r instead of the expected Keplerian decay $v \approx \sqrt{GM/r}$ predicted by a balance of the gravitational GM/r^2 and centrifugal v^2/r accelerations.

Our focus in this letter is on the structure and dynamics of disk galaxies. In the conventional picture, disk galaxies have two distinct components – a massive, three dimensional, cold dark matter (CDM) halo, and a thin '2d' disk, containing stars/gas (baryons) that is in rotational equilibrium in the combined gravitational field of the halo and the disk.

While the CDM model for dark matter works remarkably well on cosmological scales, no DM particle has yet been definitively identified. Additionally, there are several discrepancies between CDM predictions and observations on galactic or smaller scales [6]. N-body simulations give halos with the "universal" Navarro-Frenk-White (NFW) profile $\rho_{\rm NFW}(R) = \frac{\rho_0}{[(1+(R/R_S)^2)(R/R_s)]}$ [7], (R is the 3d radial coordinate). Observations, however, favor "cored" halos, e.g. the quasi-isothermal profile $\rho_{\rm qiso} = \frac{\rho_0}{(1+R^2/R_C^2)}$, over the "cuspy" NFW profile [8].

A proxy for the distribution of baryonic matter in disk galaxies is given by the surface brightness profile. In the disks of galaxies, i.e. outside the bulge if one is present, the brightness decays (approximately) exponentially from the center [9]. Assuming a constant mass-to-light ratio, the baryonic surface density $\Sigma = \Sigma_0 \exp(-r/r_0)$, where r is the 2d radial coordinate in the galactic plane, Σ_0 is the (extrapolated) central surface density and r_0 is the (baryonic) scale length of the galaxy. The Freeman "law" is observational evidence that $\Sigma_0 \approx \Sigma^*$ is the same for all high surface brightness (HSB) galaxies, *independent of their total mass* [9]. Including low surface brightness (LSB) galaxies gives a wider distribution of central densities, with a rapid fall-off beyond Σ^*, defining the *Freeman limit* [10].

Observations reveal tight correlations and scaling relations between the halo parameters ρ_0, R_C and the baryonic parameters Σ_0, r_0 [11,12]. Indeed, galaxies are *surprisingly simple* and seemingly governed by a single dimensionless parameter [13]. Since galaxy formation is inherently stochastic this suggests an important role for self-organizing dynamical processes [14].

For quasi-steady systems, many observations indicate that the dynamically inferred DM halo is strongly correlated with the baryon distribution [15]. Many of these relations are subsumed by the radial acceleration relation (RAR) [16], which is a "local" relation for the observed total acceleration $g_{\rm obs}$ (from halo + disk) and the purely baryonic contribution $g_{\rm bar}$. This relation holds for

* Corresponding author.
E-mail addresses: shankar@math.arizona.edu (S.C. Venkataramani), anewell@math.arizona.edu (A.C. Newell).

https://doi.org/10.1016/j.physletb.2020.136060

a range of galaxies including dSphs, disk galaxies (S0 to dIrr) and giant ellipticals, and was first proposed in [17] as the basis for 'Modified Newtonian dynamics (MOND)'. The successes of MOND in predicting various observed regularities on galactic scales [18] have inspired interesting proposals for coupling baryons and DM [19] as well as a variety of dark matter models that behave like MOND for galaxies and like CDM on cluster and larger scales [20,21]. There have also been attempts to recover these scaling relations within ΛCDM using cosmological simulations that include various baryonic feedback mechanisms [22,23].

Our aim in this letter is to propose specific self-organizing mechanisms for galactic dynamics. To this end, we present a theory that allows us to compute rotation curves of galaxies, and explain observed galaxy scaling relations including the RAR and the Freeman limit. We are motivated in this endeavor by the self-organizing properties of pattern forming systems and a recognition that instability generated patterns might have a role to play in galaxies [14]. In many situations, pattern structures are topologically constrained by the presence of defects and are not ground states. Therefore they can store energy. By coupling the defects to the distribution of baryons, we get additional energy that can give rise to forces that produce effects attributed to dark matter halos. In such a scenario, it is certainly plausible that there should be correlations and scaling relations between the halo and baryonic parameters.

2. Patterns, universality, defects and halos

Patterns are ubiquitous in nature and arise when, at some stress threshold, a symmetric "ground state" destabilizes and certain symmetry-breaking modes are preferentially amplified. These modes compete for dominance through nonlinear interactions and a set of winning configurations emerges. Generally, whereas some symmetries are broken, others are not, leading to the presence of defects that prevent the new state from being a ground state, a true energy minimum.

A useful illustration is provided by the well-studied case of high Prandtl number convection in a horizontal layer of fluid heated from below. For a sufficiently large thermal gradient, the conduction state becomes unstable to convective rolls which transport heat more efficiently. At this transition the continuous translation symmetry of the conductive state is broken and replaced by a discrete translation symmetry from the preferred wavelength of the roll pattern. The preferred wavelength depends only on a globally defined parameter – the Rayleigh number. However, because the rotational symmetry is not broken at the transition, the orientations of the roll patches are chosen by local biases, boundary conditions and other constraints.

If the system size is much greater than the chosen wavelength, the resulting pattern is a mosaic of "locally" uniform stripe patterns with different orientations which meet and meld along defect lines and points in 2D (and planes and loops in 3D). In more confined geometries such as cylinders or spheroids where the boundaries may be heated, or in situations where angular momentum conservation constraints might apply, the patterns, although locally stripe-like, can be target or spiral shaped. The resulting defects have topological charges reflecting the far-field geometry or constraints away from the defects. They also have energy, associated with the fact that the emerging pattern is not a true energy minimum but a metastable state; metastable in the sense that either the topological constraints make the state a local minimum or that the time scale to coarsen and "heal" the defects is extremely long.

Patterns and other collective phenomena are studied using macroscopic *order parameters* that measure the amount of symmetry breaking. Order parameters are governed by universal equations that reflect the underlying symmetries of the system but are insensitive to the precise details of the microscopic interactions in the system – a phenomenon called *universality* [24]. For systems that form stripe patterns by breaking translation but not orientation invariance, the appropriate order parameter is a phase ψ whose gradient $\mathbf{k}$ gives the local orientation of the pattern. The microscopic fields are generally 2π periodic functions of the phase ψ. Integrating over the microscopic degrees of freedom gives a canonical form for the effective energy [25]

$$\mathcal{E} = \frac{\Sigma^* c^2}{k_0^3} \int \left[(k_0^2 - \mathbf{k}^2)^2 + (\nabla \cdot \mathbf{k})^2 \right] dV, \quad \mathbf{k} = \nabla\psi, \tag{1}$$

where ψ is dimensionless, the preferred wavenumber $|\mathbf{k}| = k_0$, Σ^* is a (universal) surface density [12,15], and the normalizing constant $\frac{\Sigma^* c^2}{k_0^3}$ ensures dimensional consistency. Specifically, we will take $\Sigma^* \approx 136\, M_\odot/\mathrm{pc}^2$ corresponding to an acceleration scale $a_0 = 2\pi G \Sigma^* \approx 1.2 \times 10^{-10} \mathrm{m/s}^2$, the empirically observed universal acceleration scale in disk galaxies [17]. The ground states $\mathcal{E} = 0$ correspond to the plane waves $\psi(\mathbf{x}) = \mathbf{k}\cdot\mathbf{x}$, $|\mathbf{k}| = k_0$. If boundaries or other external constraints dictate that the phase pattern be radial, $\psi(\mathbf{x}) = \psi(R)$ where $R = |\mathbf{x}|$, we cannot be in a ground state. Indeed, a calculation reveals that, minimizing $\mathcal{E}$ with $\psi = \psi(R)$, we get $\mathbf{k} \to 0$ as $R \to 0$ and $\psi(R) \to k_0 R + \text{const}$ as $R \to \infty$. These target (spirals if the instability is to waves and (1) is modified appropriately) patterns are robust because they cannot be continuously deformed into the plane wave ground states. Their curvature radii are large compared to the local pattern wavelength, so they are locally stripe like and their macroscopic energies can be represented by (1).

What is important to us here is that the target pattern has an energy density of the same form as a cored quasi-isothermal halo with $R_C \sim k_0^{-1}$. Such halos describe the dark matter distribution out to the edge of the optical disk in real galaxies, so this suggests adding a term like (1) to the Lagrangian of a galaxy can recover the effects of 'dark matter' [25,26].

The additional action from (1) leads to the flattening of rotation curves to a limiting value $v_\infty = \sqrt{32(1-\alpha)\pi G \Sigma^*/k_0}$ [26], where α is an $O(1)$ quantity whose precise value is unimportant for this letter, and will henceforth be set to 0. While this result is encouraging important questions were left unanswered - (1) What determines the parameter k_0?, (2) How do we eliminate the assumption of spherical symmetry and model more realistic disk galaxies? and, (3) What physical processes might lead to a term like (1) in the action? We address these questions in subsequent sections.

3. An effective Lagrangian for pattern dark matter

A proper formulation of our ideas requires the identification of an appropriate Lagrangian. ΛCDM is obtained from a Lagrangian that includes the Einstein-Hilbert action for the geometry of spacetime, the 'dust' matter action for CDM/baryons, and a cosmological constant term modeling dark energy. Alternative Lagrangians describe various flavors of MOND [27–29], dark matter with novel material properties – dipolar dark matter [30], superfluid dark matter [31] and fuzzy dark matter [32], as well as "non-material" alternatives like emergent gravity [33]. Our goal is to formulate an appropriate 'pattern dark matter' Lagrangian that encapsulates the physics discussed above. Our action is the sum of

$$\mathcal{S}_{EH} = \frac{c^4}{16\pi G} \int R\sqrt{-g}\, d^4x, \quad \mathcal{S}_M = \int \rho_B u^\alpha u_\alpha \sqrt{-g}\, d^4x,$$

$$\mathcal{S}_P = -\frac{\Sigma^* c^2}{k_0^3} \int \left\{ (k_0^2 - \nabla^\mu\psi\nabla_\mu\psi)^2 + (\nabla^\mu\nabla_\mu\psi)^2 \right\} \sqrt{-g}\, d^4x,$$

$$\mathcal{S}_\psi = -\int \rho_B c^2 V\left[k_0^{-2}\nabla^\beta\psi\nabla_\beta\psi\right]\sqrt{-g}d^4x, \tag{2}$$

where ∇ represents the covariant derivative and u^α is the 4-velocity of the baryonic matter with density ρ_B. The model includes the Einstein-Hilbert action $\mathcal{S}_{EH}$, the matter action $\mathcal{S}_M$, the pattern action $\mathcal{S}_P$ as motivated by (1), and the interaction term $\mathcal{S}_\psi$ motivated by the empirical observation that the dark matter halo couples to the local baryonic density ρ_B [34]. We have introduced $V(|\mathbf{k}|^2) \geq 0$, a convex potential that vanishes at $\mathbf{k} = 0$. Large values of ρ_B create "defects" in ψ, like the spherical target pattern with $\nabla\psi = 0$ at the center. $\mathcal{S}_P$ and $\mathcal{S}_\psi$ come with negative signs since they are 'potential' terms, i.e. akin to W in the action $S = \int (T - W)\, dt$ for classical particle systems.

What remains is the specification of k_0 and the potential V. Before we do so, however, we emphasize that, irrespective of the choices we are about to make, the additional terms S_p and S_ψ in the action automatically lead to three of the key outcomes that characterize the behaviors usually associated with dark matter. First, we find that the curvature term in S_p leads to an additional force which behaves as $\frac{1}{r}$ for large r and a flattening of the velocity rotation curve given by $v_\infty^2 = \frac{32\pi G\Sigma^*}{k_0}$. Second, the coupling between the pattern "dark matter" and the baryonic density leads to the Freeman limit with a maximum central surface density on the *universal* scale Σ^* for rotation supported systems. Third, the model predicts a radial acceleration relation (RAR) between the total gravitational acceleration g_{obs} and the baryonic contribution g_{bar}, that has two branches.

Our choice for k_0 is motivated by stability considerations for a differentially rotating stellar disk $v(r) = r\,\Omega(r)$. WKB analysis gives the dispersion relation for density waves [35]

$$\omega(\mathbf{k})^2 = \sigma^2\mathbf{k}^2 - 2\pi G\Sigma_B|\mathbf{k}| + \kappa^2, \quad \kappa^2 = \frac{2\Omega}{r}\frac{d}{dr}(r^2\Omega), \tag{3}$$

where σ is the radial velocity dispersion, κ is the epicyclic frequency and Σ_B is the local baryonic surface density.

Stability for a stellar disk requires that the Toomre parameter $Q = \frac{\sigma\kappa}{\pi G\Sigma_B} > 1$. A positive κ^2 implies that the specific angular momentum $r^2\Omega$ is increasing with r, and thus stabilizes the long wavelengths $k \to 0$. This is indeed Rayleigh's criterion for stability of rotating inviscid flows. Q describes the competition between the stabilizing effects from $\kappa^2 > 0$ and the destabilizing effect of self-gravitation represented by $G\Sigma_B$. $k_1(r) = \frac{\pi G\Sigma_B}{\sigma^2}$ is the "locally" preferred (fastest growing) wavenumber.

Since our model is an attempt to encode the effects of instability induced patterns and self-organization, we posit that the phase ψ in our model is connected with the clumping instability in baryons. We therefore seek to identify the pattern wavenumber in (2) with $k_1(r)$. The 'effective' action in (2) is crude in that it only allows for a 'global' wavenumber k_0, so we will set $k_0 = k_1(r_0)$ where $r_0 \sim k_0^{-1}$ is a characteristic length scale.

If the system is rotation rather than pressure supported, the random motions have to be smaller than the ordered rotational velocity $\sigma \lesssim v(r)$. Since $\kappa \sim \frac{v(r)}{r}$ in the flat portion of the rotation curve, we get, to within an $O(1)$ constant, the radial dispersion is on the scale $\sigma \sim \sqrt{\frac{GM_B}{r}}$ and $v_\infty^2 \gtrsim \frac{GM_B}{r}$ for $r \sim r_0$, the baryonic scale length, since an $O(1)$ fraction of the total mass is within this radius.

We adopt the self-organizing principle that, if $Q < 1$, the stellar disk heats up until it reaches marginal stability $Q = 1$ at a scale $r_0 \sim k_0^{-1}$. Multiplying the 'halo estimate' $v_\infty^2 = \frac{32\pi G\Sigma^*}{k_0}$ with the stability estimate $v_\infty^2 \sim \frac{GM_B}{r_0}$ we get $v_\infty^4 = 16\mu GM_B a_0$, where $a_0 = 2\pi G\Sigma^*$ and μ is an $O(1)$ constant.

A key empirical scaling relation for disk galaxies is the Baryonic Tully-Fisher relation $v_\infty^4 = GM_B a_0$ (BTFR) relating the baryonic mass M_B to v_∞ with very little scatter over a wide range of galaxies [36]. The stability analysis suggests that, despite the approximate nature of our effective Lagrangian, it is consistent with the BTFR. We can therefore obtain the effective parameter k_0 for our model, by demanding that the halo estimate $v_\infty^2 = \frac{32\pi G\Sigma^*}{k_0}$ agree with $v_\infty^4 = 2\pi GM_B\Sigma^*$. This yields

$$k_0 = 16\sqrt{2\pi\,\Sigma^*/M_B}, \tag{4}$$

a value we will henceforth adopt. We stress that we do not claim that the stability analysis constitutes a derivation of BTFR, but simply argue that it lends credence to our calibration of k_0.

4. A variational analysis of the model

Since galaxies are non-relativistic, $v_\infty \ll c$, the geometry of space-time deviates from the flat Minkowskii space at $O(\epsilon)$ where $\epsilon = \left(\frac{v_\infty}{c}\right)^2$. We obtain the (Newtonian) limit description through a principled asymptotic expansion in the small parameter ϵ. In a steady state, our system is described by the weak-field metric, $g = -(c^2 + 2\phi(\mathbf{x}))dt^2 + (1 - 2\phi(\mathbf{x})/c^2)(dx^2 + dy^2 + dz^2)$, where $\phi(\mathbf{x})$ is the total Newtonian potential. We note that $\psi, \mathbf{x}, \mathbf{k}$ are $O(1)$, the spatial velocity $\mathbf{v} = \frac{d\mathbf{x}}{dt}$ is $O(\sqrt{\epsilon})$, and ρ_B, Σ^* and ϕ are $O(\epsilon)$. We can expand the action $\mathcal{S}$ and collect terms in powers of c (equivalently ϵ) to get, $\mathcal{S} = c^2\mathcal{S}_1 + \mathcal{S}_2$,

$$\begin{aligned}
\mathcal{S}_1 &= -\int d^3\mathbf{x}dt\left[\Sigma^* k_0^{-3}[(k_0^2 - |\nabla\psi|^2)^2 + (\Delta\psi)^2] + \rho_B V(|\nabla\psi|^2)\right]\\
\mathcal{S}_2 &= \int d^3\mathbf{x}dt\left[\rho_B\left(\frac{\mathbf{v}^2}{2} - \phi\right) - \frac{|\nabla\phi|^2}{8\pi G} - 2\phi\Sigma^* k_0^{-3}\left(|\nabla\psi|^4 - k_0^4\right)\right.\\
&\quad \left. - 2\phi\left(\Sigma^* k_0^{-3}(\Delta\psi)^2 + \rho_B V'(|\nabla\psi|^2)|\nabla\psi|^2\right)\right].
\end{aligned} \tag{5}$$

This formulation is completed by prescribing the potential V.

We illustrate the procedure for analyzing the variational equations for the action in (2) by revisiting the example of spherically symmetric compact clump of matter. **Step 1:** Prescribe $\rho_B(R)$ and solve the variational equations for $\mathcal{S}_1$, i.e. a pattern formation problem. For a compact clump, and a generic potential V with a global minimum at 0, $\nabla\psi \approx 0$ within the source, so we get the target patterns that were discussed earlier. **Step 2:** With the given ρ_B and ψ computed from the previous step, solve for the gravitational potential ϕ. For a compact dense clump, $\nabla\psi \approx 0$ where $\rho_B \neq 0$, and outside the clump, $|\nabla\psi| \approx 1, \Delta\psi \approx 2R^{-1}$. Consequently, we get $\Delta\phi \approx 4\pi G(\rho_B + 8\Sigma^* k_0/(b^2 + k_0^2R^2)), b \sim O(1)$,

$$g_{\text{obs}} = \nabla\phi \approx \frac{GM_B}{R^2} + \frac{32\pi G\Sigma^*}{k_0 R}\left[1 - \frac{b}{k_0 R}\tan^{-1}\left(\frac{k_0 R}{b}\right)\right]. \tag{6}$$

Step 3: Solve for the steady state velocity from $\frac{v^2}{R} = g_{\text{obs}}$.

To model a disk galaxy, we now carry out these steps in an axisymmetric setting, where all the fields only depend on $r = \sqrt{x^2 + y^2}$ and z. The matter density $\rho_B(r, z) \approx \Sigma_B(r)\delta(z)$ is concentrated close to the galactic plane $z = 0$.

In Step 1, extremizing $\mathcal{S}_1$, we have two contributions, the pattern Lagrangian $\mathcal{S}_P$ which is an integral over all of space, and the interaction Lagrangian $\mathcal{S}_\psi = -2\pi\int\Sigma_B(r)V(|\psi_r|^2)rdr$ which is an integral over the galactic disk. Off the disk ψ satisfies the *Eikonal equation* $|\nabla\psi| = k_0$, as appropriate for stripe patterns. Using Huygens' principle, we obtain:

$$\begin{aligned}
&\psi(r, z) = \min_{s\geq 0}\left[\psi(s, 0) + k_0\sqrt{(r - s)^2 + z^2}\right]\\
\Rightarrow\quad &\psi\left[s + t\cos\theta(s), \pm t\sin\theta(s)\right] = \psi(s, 0) + k_0 t,
\end{aligned} \tag{7}$$

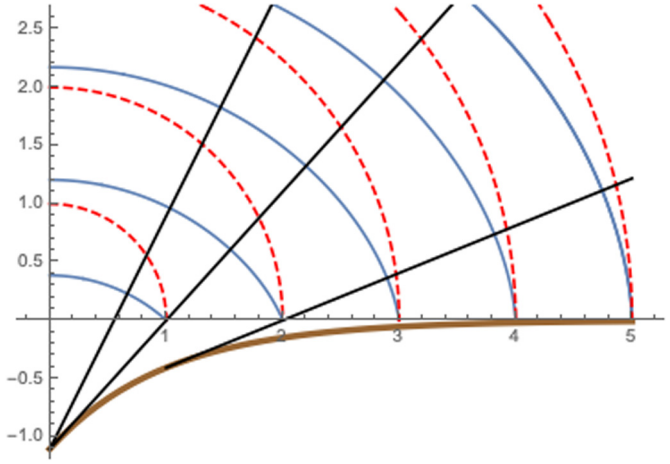

Fig. 1. Huygens' construction – the phase contours (solid curves in $z > 0$) have a common evolute (solid curve in $z < 0$) and intersect the characteristics (straight lines) orthogonally. The contours for $z \le 0$ are given by reflection. A spherical target pattern (dashed phase contours) is shown for comparison. The involutes are (approximately) spherical caps with centers off the plane $z = 0$.

where the second line follows for regions where the *characteristics* $r = s + t\cos\theta(s), z = \pm t\sin\theta(s))$ do not cross.

The geometry of this construction is illustrated in Fig. 1. The phase fronts for $z > 0$ (resp. $z < 0$) are the *involutes* of a common *evolute* $\gamma = (\alpha(s), \mp\beta(s))$ and $k_0^{-1}\psi$ is the local radius of curvature [37, §12]. For the Eikonal solution, $\nabla\psi$ is discontinuous across the galactic plane $z = 0$. Indeed, in contrast to the spherical target pattern, the contours given by the involutes intersect the plane $z = 0$ at an angle $\theta(s) \neq \frac{\pi}{2}$. This discontinuity in $\nabla\psi$ is regularized as a *phase grain boundary* (PGB), a defect well known in patterns, consisting of a boundary layer across which $\nabla\psi$ changes smoothly as illustrated in Fig. 2.

We can estimate the (surface) energy density of a PGB as follows. Since the boundary layer has width w, the curvature and stretch of the phase contours are, respectively, $\Delta\psi \sim k_0 w^{-1}\sin\theta(s)$, $k_0^2 - |\nabla\psi|^2 \sim k_0^2\sin^2\theta(s)$. Eq. (1) now implies

$$\Sigma_{PGB} \sim w^{-1}k_0^2\sin^2\theta(s) + wk_0^4\sin^4\theta(s).$$

Optimizing for w gives $w \sim \frac{1}{k_0\sin\theta(s)}$, $\Sigma_{PGB} \propto \sin^3\theta(s)$. A rigorous calculation along these lines yields $\Sigma_{PGB} = \frac{8\Sigma^*}{3}\sin^3\theta(s)$ [38]. Using (4), the sum of $\mathcal{S}_\psi$ and the PGB defect energy is

$$\mathcal{S}_{\text{disk}} = 2\pi\int\left[\frac{8\Sigma^*}{3}\sin^3\theta(s) + \Sigma_B(s)V(k_0^2\cos^2\theta(s))\right]sds. \qquad (8)$$

We can extremize to get $k_0^2\Sigma_B(s)V'(\cos^2\theta(s)) = 4\Sigma^*\sin\theta(s)$, *a local relation* between the matter surface density, the characteristic angle $\theta(s)$, and indirectly, also the common evolute γ.

We can now make an informed choice for the potential V. The argument of V is $|\nabla\psi|^2 = k_0^2\cos^2\theta(s) \le k_0^2$ within the galactic disk. To ensure $|\nabla\psi|^2 \le k_0^2$ in the presence of matter, a canonical choice is the *log barrier function* $V = -V_0\ln(k_0^2 - |\nabla\psi|^2)$ [39], where V_0 is an $O(1)$ constant. Putting everything together, we have the leading order (in $\epsilon = (v_\infty/c)^2$ small and $k_0\sqrt{r^2+z^2}$ large) solution of the variational equations for (2):

$$(r, z) = (s + t\cos\theta(s), \pm t\sin\theta(s)),$$
$$\gamma = \left(s + \frac{\cos\theta(s)\sin\theta(s)}{\theta'(s)}, \frac{\sin^2\theta(s)}{\theta'(s)}\right)$$
$$\Sigma_B(s) = \frac{4\Sigma^*}{V_0}\sin^3\theta(s)$$

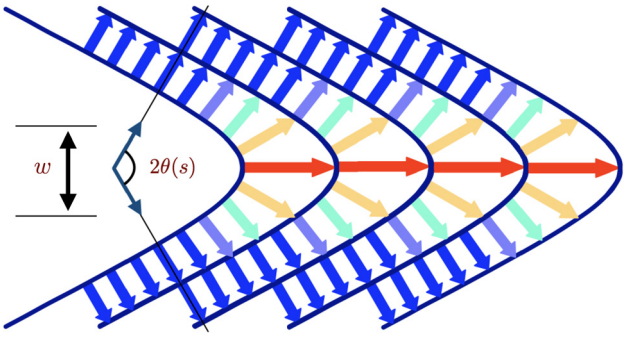

Fig. 2. Phase grain boundary (PGB). There is a jump in $\nabla\psi$ across the PGB. This structure is smooth on the scale w, the width of the PGB. The stretching and bending of the phase contours contribute to an effective surface energy.

$$|\nabla\psi| \simeq k_0, \quad \Delta\psi \simeq 2k_0\left(t - \sin\theta(s)/\theta'(s)\right)^{-1} \approx 2k_0/\sqrt{r^2+z^2},$$
$$\Delta\phi = \Delta(\phi_B + \phi_P) \simeq 4\pi G\left[\Sigma_B(r)\delta(z) + 2\Sigma^*k_0^{-3}(\Delta\psi)^2\right],$$
$$v^2 = r\partial_r\phi(r,0) = r\partial_r\phi_B(r,0) + r\partial_r\phi_P(r,0). \qquad (9)$$

The curvature of the phase contours is $\Delta\psi$ and the effective mass density in the pattern field ψ is $2\Sigma^*k_0^{-3}(\Delta\psi)^2$. The leading order solution of ψ is given by (7) as long as the curvature $\Delta\psi \lesssim k_0^2$, consistent with a 'cored dark halo'.

5. Phase surfaces as dark halos

We record a few observations. An important caveat is that our equations describe equilibria for *purely rotation supported* galaxies – no significant random motions or 3d structure, i.e. no bulge or pseudobulge. In the current form, Eqs. (9) are consequently limited to describing 'pure disk' LSB galaxies. For such galaxies, (9) implies the Freeman limit $\Sigma_B \le \frac{4\Sigma^*}{V_0}$ [10].

Although Eqs. (9) do not describe the central regions of HSB galaxies, we expect that they do describe the disk component. For HSB galaxies, the Freeman limit applies to the extrapolated central density, obtained from the exponential disk region $\Sigma_B = \Sigma_0 e^{-r/r_0}$ and not for the "true" line-of-sight central surface density, which can be substantially higher, and instead satisfies the central surface density relation CSDR [40,19]. Further work is needed to obtain these relations for HSB galaxies within our framework as this will require extending our model.

The second equation in (9) expresses the common evolute γ in terms of $\theta(s)$ which in turn is given by Σ_B. This connects the *local* matter distribution Σ_B and the pattern 'halo'.

We can also prescribe γ and use it to compute Σ_B, ψ, ϕ and v. A natural *critical* case is when the evolute degenerates to a single point $(0, -z_0)$, so that $\theta(s) = \arctan(\frac{z_0}{s})$ and $\Sigma_B(s) = \frac{4\Sigma^*}{V_0}(1 + s^2/z_0^2)^{-3/2}$, corresponding to a Kuzmin disk. It is remarkable that the surface density of a Kuzmin disk, a natural model for galactic disks, arises from the surface energy $\propto \sin^3\theta(s)$ relation for PGB defects, a formula that was originally derived in a totally different context of patterns [38].

The mass of this 'critical' Kuzmin disk, $M_B = 8\pi\Sigma^*z_0^2/V_0$, is determined by z_0, the length-scale in the evolute. The phase is given by $\psi(r,z) = k_0(r^2 + (|z| + z_0)^2)^{1/2}$ and the curvature of the contours is $1/(r^2 + (|z| + z_0)^2)^{1/2} \le z_0^{-1}$ so the eikonal approximation for the phase is valid for all (r, z). We can compute the potential $\phi(r, 0)$ and the rotation velocity:

$$\frac{\phi(r,0)}{2\pi G\Sigma^*z_0} \approx -\frac{4}{V_0\sqrt{1+\xi^2}} + V_0^{-1/2}\log(1+\xi^2) + \cdots,$$
$$\frac{v^2(r)}{2\pi G\Sigma^*z_0} \approx \frac{4\xi^2}{V_0(1+\xi^2)^{3/2}} + 2V_0^{-1/2}\frac{\xi^2}{1+\xi^2} + \cdots,$$

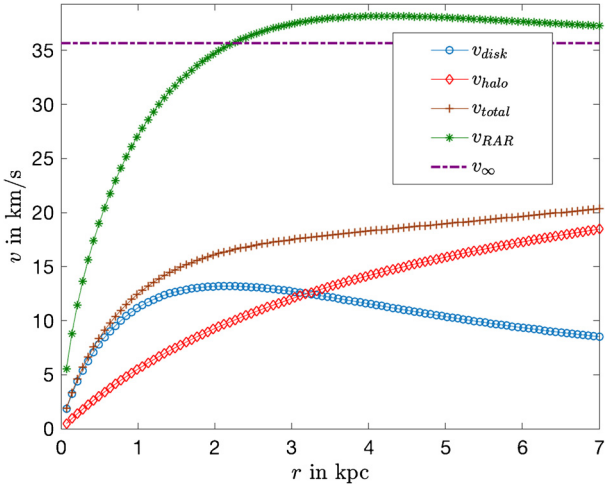

Fig. 3. Computed rotation curves. $a_0 = 3600\,\mathrm{km^2 s^{-2} kpc^{-1}}$. We approximate the pattern DM density $2\Sigma^* k_0^{-1}(\Delta\psi)^2$ by the $\ell = 0$ mode. We also plot the rotation curve obtained from Eq. (12) for the RAR. Compare Fig. 7 in Ref. [41].

$$\frac{g_{\rm obs}}{2\pi G\Sigma^*} \approx \frac{4\xi}{V_0(1+\xi^2)^{3/2}} + 2V_0^{-1/2}\frac{\xi}{1+\xi^2} + \cdots \tag{10}$$

where $\xi = r/z_0$ is the scaled radius, and the initial terms are the (non-dimensional) baryonic contributions to the potential ($\phi_{\rm bar}$), velocity ($v_{\rm disk}$) and acceleration ($g_{\rm bar}$). The asymptotic velocity $v_\infty^2 = 4\pi V_0^{-1/2} G\Sigma^* z_0 \equiv (GM_B a_0)^{1/2}$ where $a_0 = 2\pi G\Sigma^*$. Independent of the scale z_0, the critical Kuzmin disks in our theory satisfy a radial acceleration relation (RAR) since both $\frac{g_{\rm bar}}{a_0}$ and $\frac{g_{\rm obs}}{a_0}$ only depend on the combination $\xi = r/z_0$.

While the Kuzmin disk is a useful model, most real galaxies are exponential disks [9]. Interestingly, exponential disks also arise naturally in our theory. From (9), a "limiting" case for a cored halo corresponds to $\theta'(s) = z_0^{-1}\sin\theta(s)$ which ensures that $\Delta\psi \geq 2k_0 z_0^{-1}$. Solving for $\theta(s)$ and computing the corresponding density Σ_B using (9), we get,

$$\Sigma_B(s) = \frac{4\Sigma^* A^3}{V_0}\frac{e^{-3s/z_0}}{(1+A^2 e^{-2s/z_0}/4)^3}. \tag{11}$$

For $A \lesssim 1$, this is the baryonic density of an exponential disk $\Sigma_B = \Sigma_0 e^{-s/r_0}$ with $\Sigma_0 = \frac{4\Sigma^* A^3}{V_0}$, $r_0 = \frac{1}{3}z_0$, suggesting that the self-organizing processes underlying our model might naturally produce exponential disks if the dynamics drive the phase curvatures to a constant (maximal) value on the galactic plane.

Rather than attempting to explain the origins of exponential profiles for disk galaxies, our goal here is somewhat more limited, namely, we seek to compute the rotation curves for LSB exponential disks within our theory. We henceforth set $V_0 = 4$. Combining (11) and (4) we obtain $k_0 z_0 = 48\,A^{-3/2}$. Fig. 3 shows the numerically obtained rotation curves for a model exponential disk with $r_0 = 1\,\mathrm{kpc}$, $M_B = 10^8 M_\odot$ corresponding to $A \approx 1/2$. The rotation curve computed from our theory rises slowly, and continues to rise beyond $7r_0$. The shape of the curve as well as the scale of the velocity is in good qualitative agreement with the observational curves in [41].

In Fig. 4, we plot the RAR for our theory applied to various matter distributions (V_0 is set to 4) and compare with the fit

$$g_{\rm obs} = \frac{g_{\rm bar}}{1 - e^{-\sqrt{g_{\rm bar}/g_\dagger}}} \tag{12}$$

for the choice $g_\dagger = a_0$ [16]. Note that, for rotation supported systems, the resulting RAR has two branches. In the absence of a bulge/central mass, the baryonic contribution to the acceleration

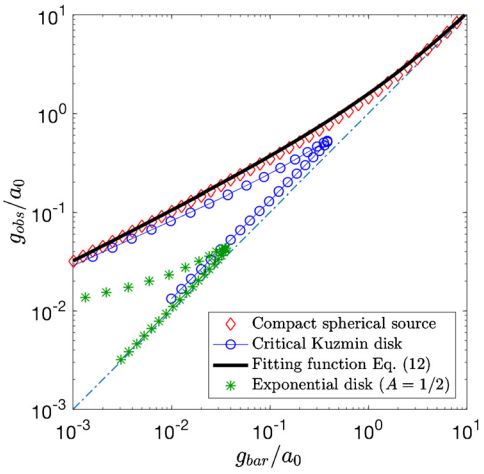

Fig. 4. The radial acceleration relation (RAR) in our model for various distributions of matter. $g_{\rm obs}$ and $g_{\rm bar}$ are the total gravitational acceleration and the baryonic contribution respectively. No parameters are fit: $g_\dagger = a_0 = 2\pi G\Sigma^*$. Compare Fig. 1 in Ref. [42].

$g_{\rm bar}$ has a peak value $g_{\rm max}$ at a few scale-lengths. For $g < g_{\rm max}$ there are two values of r, one on either side of the peak, with $g_{\rm bar}(r) = g$ and (generically) *different* values of $g_{\rm obs}$, giving two branches that meet at the peak acceleration. Our theory therefore gives two branches for the RAR in agreement with recent observations for dwarf disk and LSB galaxies [42].

Fig. 3 illustrates the comparison between the RAR prediction, using (12) and $\frac{v^2}{r} = g_{\rm obs}$, with the rotation curve from our model. While the RAR prediction peaks and then declines slightly, the rotation curve given by (9) continues to rise, albeit slowly. The RAR prediction and our computed curve will both asymptote to the same value v_∞ given by the BTFR. However, this, clearly, *does not* determine the entire rotation curve, which therefore serves as a test for the validity of our theory, even allowing for the (nonlocal) calibration for k_0 in (4).

Importantly, the discrepancies between our predictions and the RAR are significant in the 'inner' regions (within a scale length). Besides the difficulties in resolving the rotation curves on these scales, this region is strongly influenced by the galactic bulge and/or a central black hole (if present). In particular, if the baryonic acceleration $g_{\rm bar}$ is monotonically decreasing in the region that can be resolved by observations, it is likely that $g_{\rm obs}$ will be a monotonic function of $g_{\rm bar}$ and discrepancies between our model and the RAR given by (12) might be hard to detect.

6. Discussion

We have proposed an effective Lagrangian theory for dark matter, by combining ideas from pattern formation with empirical observations. We have introduced an additional "dark field" ψ that plays the role of DM. In our theory, no structures are formed on scales smaller than k_0^{-1} resulting in cored DM halos in contrast to the cuspy halos formed by CDM.

Our theory is based on universal equations for pattern formation and can thus describe a variety of instability generating mechanisms. Our favored interpretation is that ψ is the order parameter for a broken translational symmetry, with a characteristic scale k_0^{-1} determined by the distribution of baryons. We identify k_0 with the most unstable wavenumber in the stability analysis that leads to Toomre's criterion [35], thereby directly relating the 'baryonic instability' of a rotating disk to the pattern instability that produces the 'dark halo' in our framework.

Ours is an effective, long wave theory, applicable on scales $\gtrsim k_0^{-1}$, rather than a fundamental theory, since k_0 in (2) explicitly

depends on the baryonic mass M_B of the host galaxy, as given by Eq. (4). This nonlocality is to be expected and is indeed unavoidable for an effective theory that is consistent with the BTFR [43]. Our theory is "minimally" nonlocal through the dependence of its action on a single global quantity M_B.

With no additional fitting parameters, our parsimonious theory retrodicts some of the observed regularities and scaling laws for isolated, quasi-steady, rotation supported systems, including the RAR and the existence of the Freeman limit.

There are two distinct sources for the new effects arising in our theory. First, the curvature of the phase surfaces contributes an additional energy (mass), consistent with cored halos. The resulting gravitational acceleration dominates the baryonic contribution g_{bar} at large distances and flattens the rotation curves. Second, for disk galaxies, the phase surfaces are spheroidal rather than spherical and thus generate a phase grain boundary on the galactic plane. This additional source yields the third relation in Eq. (9), linking $\theta(s)$, the angle between the phase surfaces and the galactic plane, to the density of the disk, $\Sigma(s)$, providing a natural explanation for the disk-halo connection in galaxies [34,41]. One consequence of this connection is that exponential disks correspond to a constant curvature for the phase surfaces on the galactic disk $z = 0$, and thus to a constant 'halo' surface density [12].

A limitation of our current analysis is that it does not apply to bulges, elliptic galaxies or other pressure supported systems. In ongoing work we are investigating the use of a perfect fluid in place of the dust Lagrangian for matter in Eq. (2), to extend our analysis to systems with pressure supported components. We are also evaluating the consequences of the potential instability of the PGB when the angle $\theta(s)$ becomes too sharp [38].

Galaxy formation is a complex process, and involves a great many effects [44,45] not included in our simple model. In cosmological contexts galaxies are "nonlinear", with the implication sometimes being that theorists can build models that describe the very largest scales of the universe, and not be too concerned with tensions between theories and observations, or "unexplained" regularities/scaling laws, on small "nonlinear" scales [15]. We disagree with this point of view. We contend that the robust scaling relations satisfied by galaxies are not "accidental" and require robust explanations. Our model offers conceptual insight into these relations by demonstrating how a generic mechanism for coupling the dark field ψ, through its defects, to the baryonic density ρ_B leads to self-organization.

Our model allows us to compute the rotation curves of exponential disk galaxies. The resulting phase contours for exponential disks are (approximately) spherical caps $\psi \approx (r^2 + (z + z_0)^2)^{1/2}$, as illustrated in Fig. 1, implying that the Kuzmin disk solutions approximate the "dark halos" of disk galaxies [46]. This *universality* [24] justifies our use of simplified physical models, with relatively few ingredients, in this preliminary attempt to understand self-organization in galaxies.

Declaration of competing interest

The authors declare that they have no known competing financial interests or personal relationships that could have appeared to influence the work reported in this paper.

Acknowledgements

We are grateful to Peter Behroozi and Stacy McGaugh for many illuminating discussions, and to an anonymous referee for many valuable comments. SCV was partially supported by the Simons Foundation through award 524875 and by the National Science Foundation through award DMR-1923922. SCV and ACN were also partially supported by National Science Foundation GCR-2020915.

References

[1] V. Trimble, Existence and nature of dark matter in the universe, Annu. Rev. Astron. Astrophys. 25 (1987) 425–472, https://doi.org/10.1146/annurev.aa.25.090187.002233.
[2] J.H. Oort, The force exerted by the stellar system in the direction perpendicular to the galactic plane and some related problems, Bull. Astron. Inst. Neth. 6 (1932) 249.
[3] F. Zwicky, Die Rotverschiebung von extragalaktischen Nebeln, Helv. Phys. Acta 6 (1933) 110–127.
[4] V.C. Rubin, W.K. Ford Jr., Rotation of the Andromeda Nebula from a spectroscopic survey of emission regions, Astrophys. J. 159 (1970) 379, https://doi.org/10.1086/150317.
[5] V.C. Rubin, N. Thonnard, W.K. Ford Jr., Extended rotation curves of high-luminosity spiral galaxies. IV - Systematic dynamical properties, SA through SC, Astrophys. J. Lett. 225 (1978) L107–L111, https://doi.org/10.1086/182804.
[6] I. de Martino, S.S. Chakrabarty, V. Cesare, A. Gallo, L. Ostorero, A. Diaferio, Dark matters on the scale of galaxies, Universe 6 (8) (2020) 107.
[7] J.F. Navarro, C.S. Frenk, S.D.M. White, The structure of cold dark matter halos, Astrophys. J. 462 (1996) 563, https://doi.org/10.1086/177173, arXiv:astro-ph/9508025.
[8] P. Li, F. Lelli, S. McGaugh, J. Schombert, A comprehensive catalog of dark matter halo models for SPARC galaxies, Astrophys. J. Suppl. Ser. 247 (1) (2020) 31, https://doi.org/10.3847/1538-4365/ab700e.
[9] K.C. Freeman, On the disks of spiral and S0 galaxies, Astrophys. J. 160 (1970) 811, https://doi.org/10.1086/150474.
[10] S.S. McGaugh, G.D. Bothun, J.M. Schombert, Galaxy selection and the surface brightness distribution, Astron. J. 110 (1995) 573, https://doi.org/10.1086/117543, arXiv:astro-ph/9505062.
[11] F. Donato, G. Gentile, P. Salucci, Cores of dark matter haloes correlate with stellar scalelengths, Mon. Not. R. Astron. Soc. 353 (2) (2004) L17–L22, https://doi.org/10.1111/j.1365-2966.2004.08220.x.
[12] F. Donato, G. Gentile, P. Salucci, C. Frigerio Martins, M.I. Wilkinson, G. Gilmore, E.K. Grebel, A. Koch, R. Wyse, A constant dark matter halo surface density in galaxies, Mon. Not. R. Astron. Soc. 397 (3) (2009) 1169–1176, https://doi.org/10.1111/j.1365-2966.2009.15004.x.
[13] M.J. Disney, J.D. Romano, D.A. Garcia-Appadoo, A.A. West, J.J. Dalcanton, L. Cortese, Galaxies appear simpler than expected, Nature 455 (7216) (2008) 1082–1084, https://doi.org/10.1038/nature07366.
[14] M.J. Aschwanden, F. Scholkmann, W. Béthune, W. Schmutz, V. Abramenko, M.C.M. Cheung, D. Müller, A. Benz, G. Chernov, A.G. Kritsuk, J.D. Scargle, A. Melatos, R.V. Wagoner, V. Trimble, W.H. Green, Order out of randomness: self-organization processes in astrophysics, Space Sci. Rev. 214 (2) (2018) 55, https://doi.org/10.1007/s11214-018-0489-2.
[15] B. Famaey, S.S. McGaugh, Modified Newtonian dynamics (MOND): observational phenomenology and relativistic extensions, Living Rev. Relativ. 15 (1) (2012) 10, https://doi.org/10.12942/lrr-2012-10.
[16] F. Lelli, S.S. McGaugh, J.M. Schombert, M.S. Pawlowski, One law to rule them all: the radial acceleration relation of galaxies, Astrophys. J. 836 (2) (2017) 152, https://doi.org/10.3847/1538-4357/836/2/152, arXiv:1610.08981.
[17] M. Milgrom, A modification of the Newtonian dynamics as a possible alternative to the hidden mass hypothesis, Astrophys. J. 270 (1983) 365–370, https://doi.org/10.1086/161130.
[18] S. McGaugh, Predictions and outcomes for the dynamics of rotating galaxies, Galaxies 8 (2) (2020) 35, https://doi.org/10.3390/galaxies8020035.
[19] B. Famaey, J. Khoury, R. Penco, A. Sharma, Baryon-interacting dark matter: heating dark matter and the emergence of galaxy scaling relations, J. Cosmol. Astropart. Phys. 2020 (06) (2020) 025, https://doi.org/10.1088/1475-7516/2020/06/025.
[20] H. Zhao, B. Li, Dark fluid: a unified framework for modified Newtonian dynamics, dark matter, and dark energy, Astrophys. J. 712 (1) (2010) 130–141, https://doi.org/10.1088/0004-637x/712/1/130.
[21] J. Khoury, Alternative to particle dark matter, Phys. Rev. D 91 (2015) 024022, https://doi.org/10.1103/PhysRevD.91.024022, https://link.aps.org/doi/10.1103/PhysRevD.91.024022.
[22] J.F. Navarro, A. Benítez-Llambay, A. Fattahi, C.S. Frenk, A.D. Ludlow, K.A. Oman, M. Schaller, T. Theuns, The origin of the mass discrepancy-acceleration relation in ΛCDM, Mon. Not. R. Astron. Soc. 471 (2) (2017) 1841–1848, https://doi.org/10.1093/mnras/stx1705, arXiv:1612.06329.
[23] A.A. Dutton, A.V. Macciò, A. Obreja, T. Buck, NIHAO – XVIII. Origin of the MOND phenomenology of galactic rotation curves in a ΛCDM universe, Mon. Not. R. Astron. Soc. 485 (2) (2019) 1886–1899, https://doi.org/10.1093/mnras/stz531.
[24] L.P. Kadanoff, Scaling and universality in statistical physics, Phys. A, Stat. Mech. Appl. 163 (1) (1990) 1–14, https://doi.org/10.1016/0378-4371(90)90309-G.
[25] A.C. Newell, S.C. Venkataramani, Elastic sheets, phase surfaces, and pattern universes, Stud. Appl. Math. 139 (2) (2017) 322–368, https://doi.org/10.1111/sapm.12184.
[26] A.C. Newell, S.C. Venkataramani, Pattern universes, C. R., Méc. 347 (4) (2019) 318–331, https://doi.org/10.1016/j.crme.2019.03.004.

[27] J. Bekenstein, M. Milgrom, Does the missing mass problem signal the breakdown of Newtonian gravity?, Astrophys. J. 286 (1984) 7–14, https://doi.org/10.1086/162570.
[28] J.D. Bekenstein, Relativistic gravitation theory for the modified Newtonian dynamics paradigm, Phys. Rev. D 70 (2004) 083509, https://doi.org/10.1103/PhysRevD.70.083509, https://link.aps.org/doi/10.1103/PhysRevD.70.083509.
[29] C. Skordis, T. Złosnik, A new relativistic theory for Modified Newtonian Dynamics, arXiv e-prints, arXiv:2007.00082, 2020.
[30] L. Blanchet, L. Heisenberg, Dipolar dark matter as an effective field theory, Phys. Rev. D 96 (2017) 083512, https://doi.org/10.1103/PhysRevD.96.083512, https://link.aps.org/doi/10.1103/PhysRevD.96.083512.
[31] L. Berezhiani, J. Khoury, Theory of dark matter superfluidity, Phys. Rev. D 92 (2015) 103510, https://doi.org/10.1103/PhysRevD.92.103510.
[32] W. Hu, R. Barkana, A. Gruzinov, Fuzzy cold dark matter: the wave properties of ultralight particles, Phys. Rev. Lett. 85 (2000) 1158–1161, https://doi.org/10.1103/PhysRevLett.85.1158.
[33] S. Hossenfelder, Covariant version of Verlinde's emergent gravity, Phys. Rev. D 95 (2017) 124018, https://doi.org/10.1103/PhysRevD.95.124018, https://link.aps.org/doi/10.1103/PhysRevD.95.124018.
[34] R. Sancisi, The visible matter – dark matter coupling, Symp. - Int. Astron. Union 220 (2004) 233–240, https://doi.org/10.1017/S0074180900183299.
[35] A. Toomre, On the gravitational stability of a disk of stars, Astrophys. J. 139 (1964) 1217–1238, https://doi.org/10.1086/147861.
[36] S.S. McGaugh, J.M. Schombert, G.D. Bothun, W.J.G. de Blok, The baryonic Tully-Fisher relation, Astrophys. J. Lett. 533 (2) (2000) L99–L102, https://doi.org/10.1086/312628, arXiv:astro-ph/0003001.
[37] J. Rutter, Geometry of Curves, Chapman & Hall/CRC, Boca Raton, Fla, 2000.
[38] A.C. Newell, T. Passot, C. Bowman, N. Ercolani, R. Indik, Defects are weak and self-dual solutions of the Cross-Newell phase diffusion equation for natural patterns, Phys. D: Nonlinear Phenom. 97 (1) (1996) 185–205.
[39] S. Boyd, L. Vandenberghe, Convex Optimization, Cambridge University Press, Cambridge UK, New York, 2004.
[40] F. Lelli, S.S. McGaugh, J.M. Schombert, M.S. Pawlowski, The relation between stellar and dynamical surface densities in the central regions of disk galaxies, Astrophys. J. 827 (1) (2016) L19, https://doi.org/10.3847/2041-8205/827/1/l19.
[41] C. Di Paolo, P. Salucci, A. Erkurt, The universal rotation curve of low surface brightness galaxies - IV. The interrelation between dark and luminous matter, Mon. Not. R. Astron. Soc. 490 (4) (2019) 5451–5477, https://doi.org/10.1093/mnras/stz2700, arXiv:1805.07165.
[42] C. Di Paolo, P. Salucci, J.P. Fontaine, The radial acceleration relation (RAR): crucial cases of dwarf disks and low-surface-brightness galaxies, Astrophys. J. 873 (2) (2019) 106, https://doi.org/10.3847/1538-4357/aaffd6.
[43] C. Deffayet, G. Esposito-Farèse, R.P. Woodard, Nonlocal metric formulations of modified Newtonian dynamics with sufficient lensing, Phys. Rev. D 84 (2011) 124054, https://doi.org/10.1103/PhysRevD.84.124054.
[44] J.J. Dalcanton, D.N. Spergel, F.J. Summers, The formation of disk galaxies, Astrophys. J. 482 (2) (1997) 659–676, https://doi.org/10.1086/304182, arXiv:astro-ph/9611226.
[45] R.H. Wechsler, J.L. Tinker, The connection between galaxies and their dark matter halos, Annu. Rev. Astron. Astrophys. 56 (1) (2018) 435–487, https://doi.org/10.1146/annurev-astro-081817-051756.
[46] R. Brada, M. Milgrom, Exact solutions and approximations of MOND fields of disc galaxies, Mon. Not. R. Astron. Soc. 276 (2) (1995) 453–459, https://doi.org/10.1093/mnras/276.2.453.